

**Simultaneous Purification and Surface Plasmon Resonance
Characterization of Mechanoresponsive, Discretely
Functionalized Gold Nanoparticles**

Chun-Pong Chak, Long-Ho Chau, Shu-Yuen Wu, Ho-Pui Ho, Wen J. Li,

*Paula M. Mendes and Ken Cham-Fai Leung**

Supplementary Information

*Corresponding author

Prof. Ken Cham-Fai Leung
Center of Novel Functional Molecules
and Institute of Molecular Functional Materials
Department of Chemistry
The Chinese University of Hong Kong
Shatin, NT, Hong Kong SAR, P. R. China.
Phone: (+852) 2609 6342
Fax: (+852) 2603 5057
E-mail: cfleung@cuhk.edu.hk

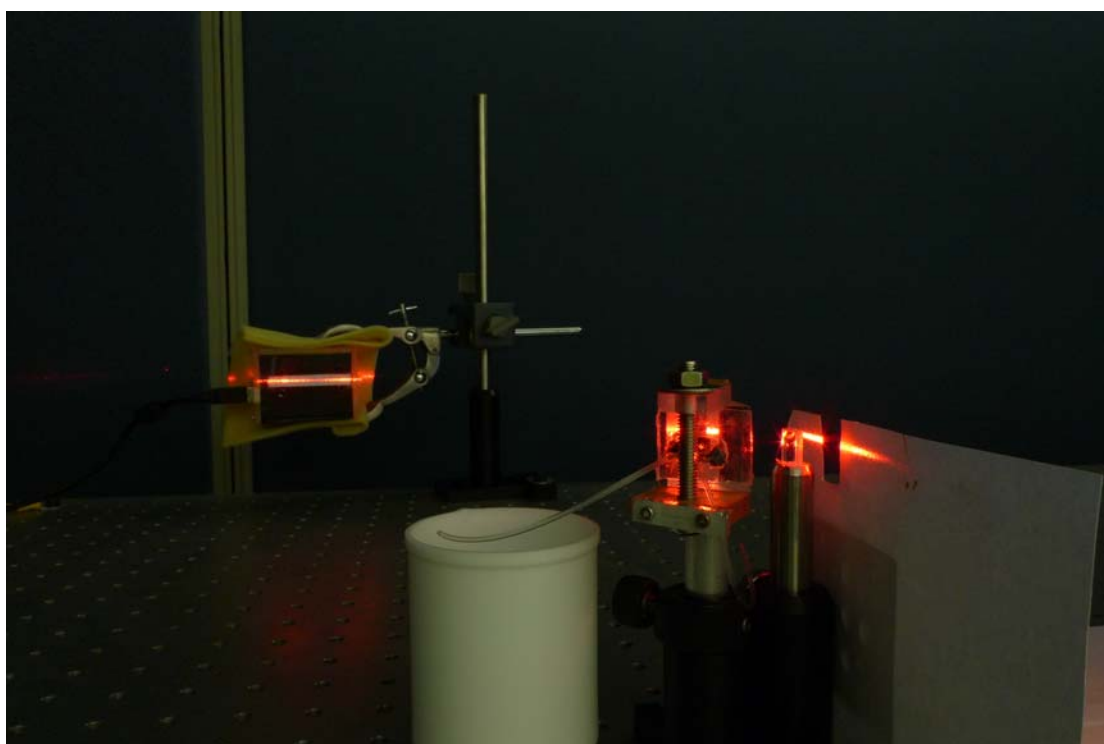
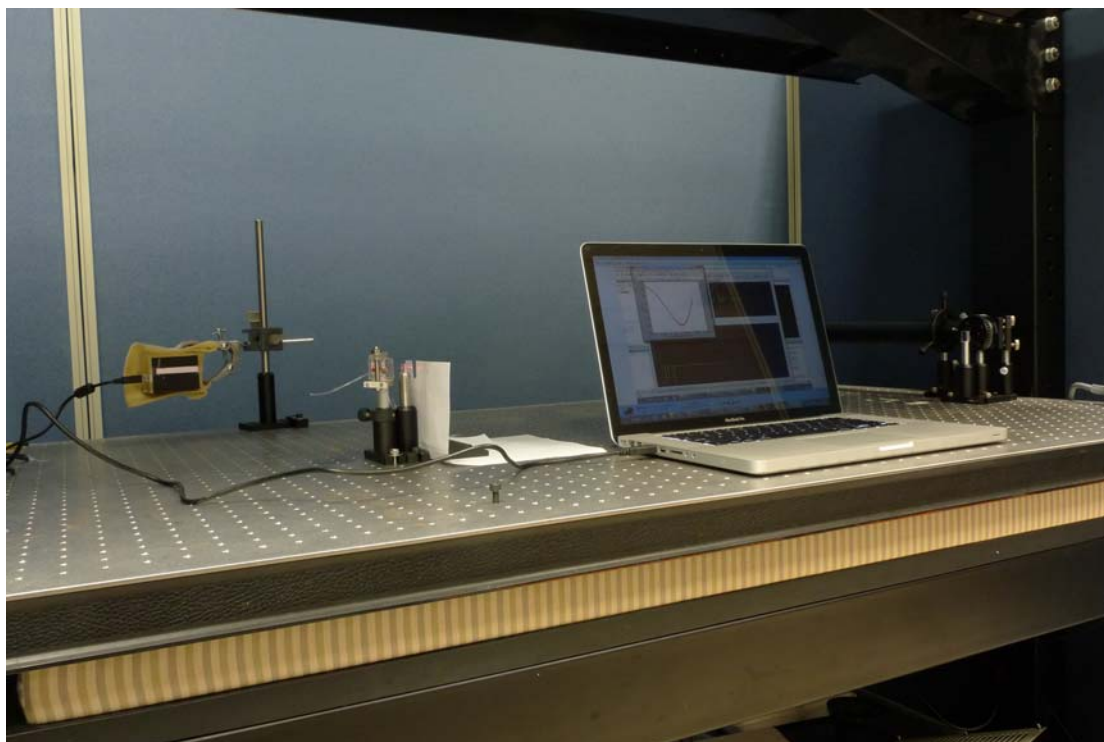


Figure S1. Experimental set-up of the surface plasmon resonance (SPR) device equipped with microfluidic system.

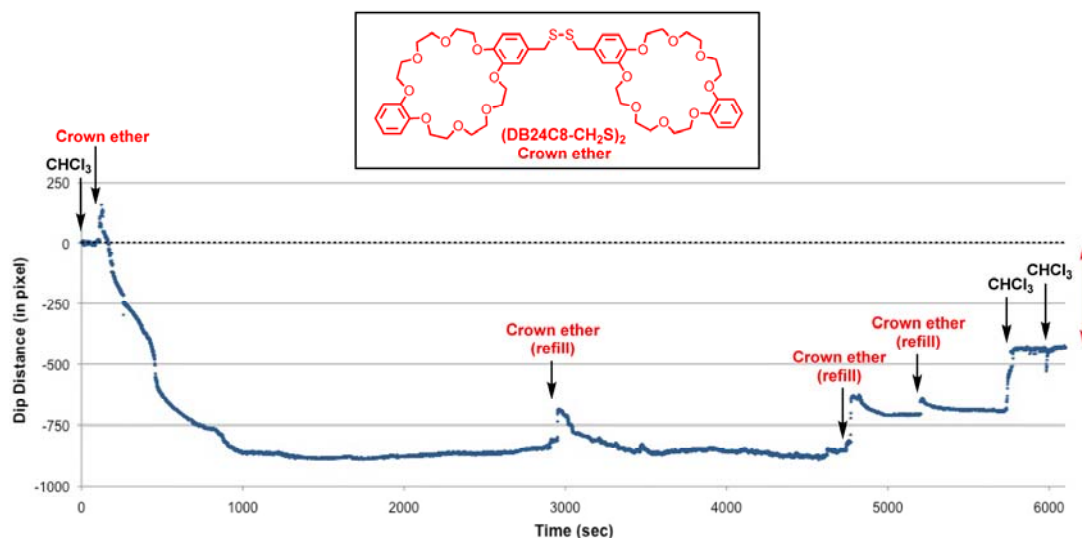


Figure S2. Real-time SPR trace of crown ether derivatization onto gold surface. The final dip distance was approximately -430 pixels (red arrow) after extensive washing with solvent. This result revealed that a layer of crown ether was successfully conjugated to the gold surface.

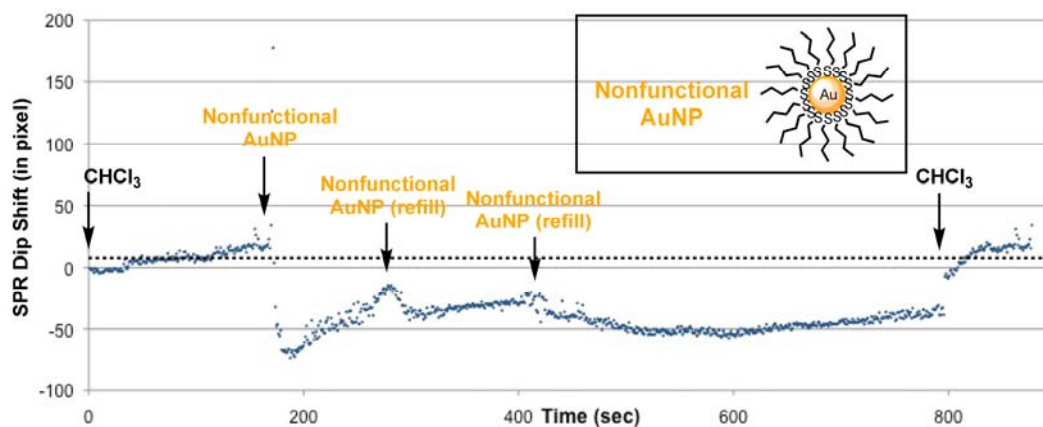


Figure S3. Real-time SPR trace when nonfunctional gold nanoparticles were added onto the crown ether-coated gold surface. After extensive washing with solvent, the dip distance returned to zero pixel, demonstrating that gold nanoparticles were neither self-assembled nor physisorbed onto the crown ether-coated gold surface.

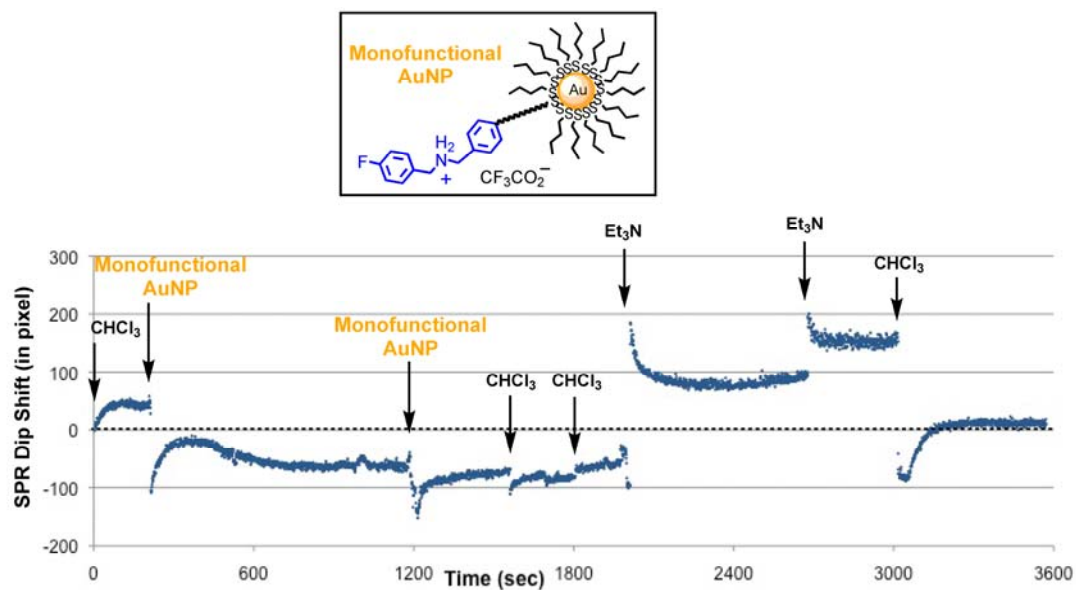


Figure S4. Additional real-time SPR trace for the pH-driven self-assembly of monofunctional gold nanoparticles onto the crown ether-coated gold surface.

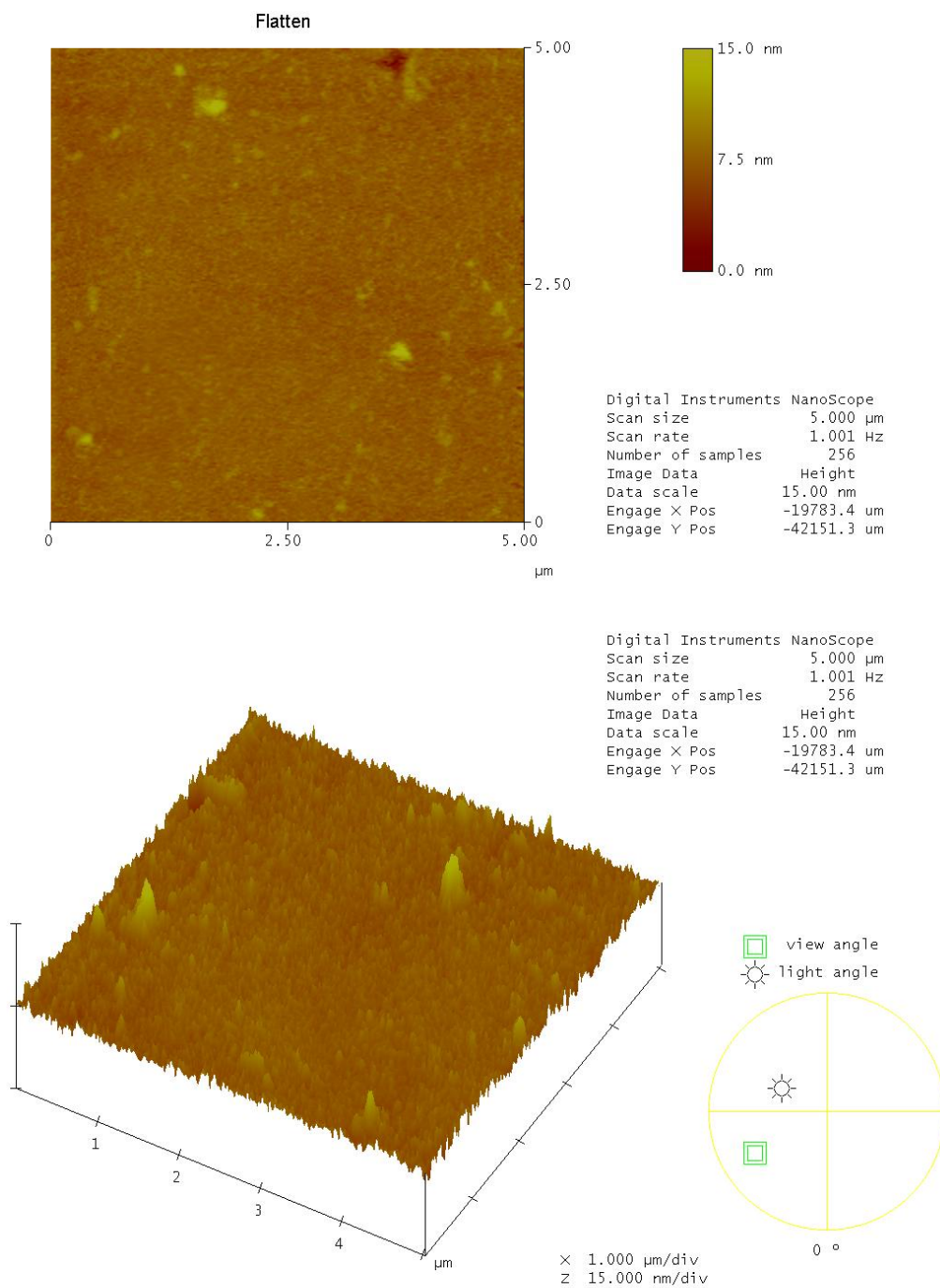


Figure S5. Additional AFM images of crown ether-coated gold surface.

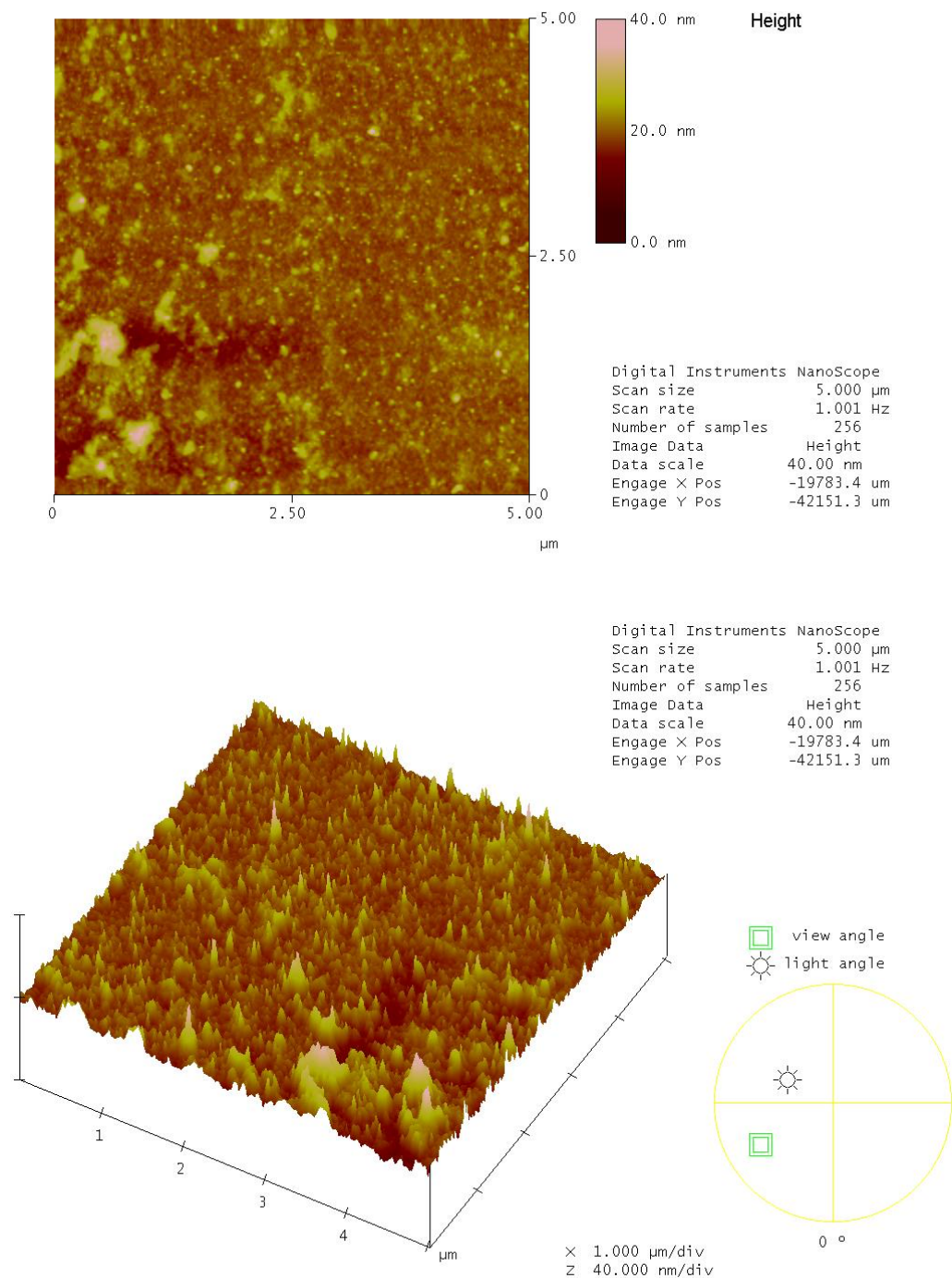


Figure S6. Additional AFM images of crown ether-coated gold surface self-assembled with monofunctional gold nanoparticles.

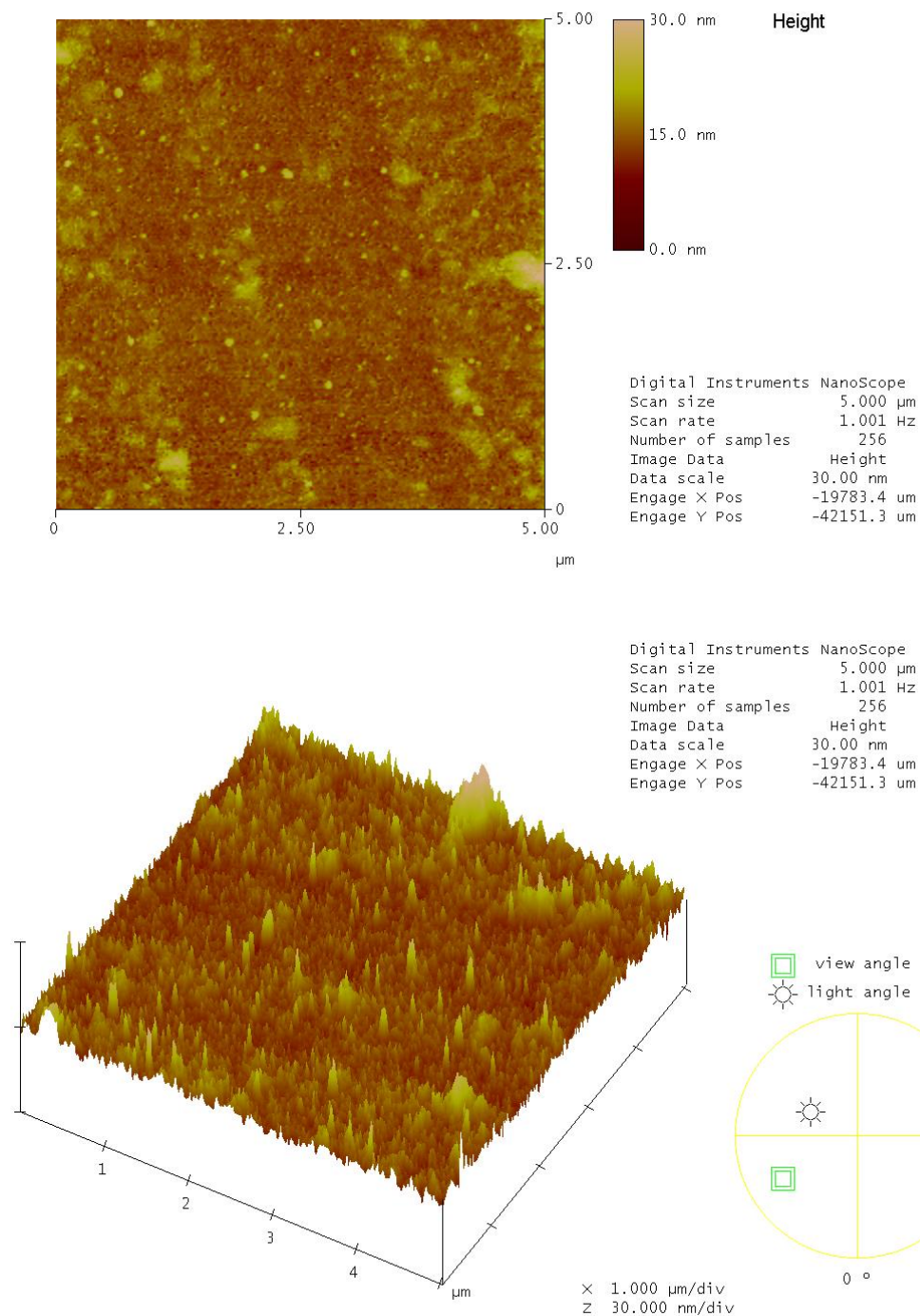


Figure S7. Additional AFM images of crown ether-coated gold surface self-assembled with randomly functional gold nanoparticles.

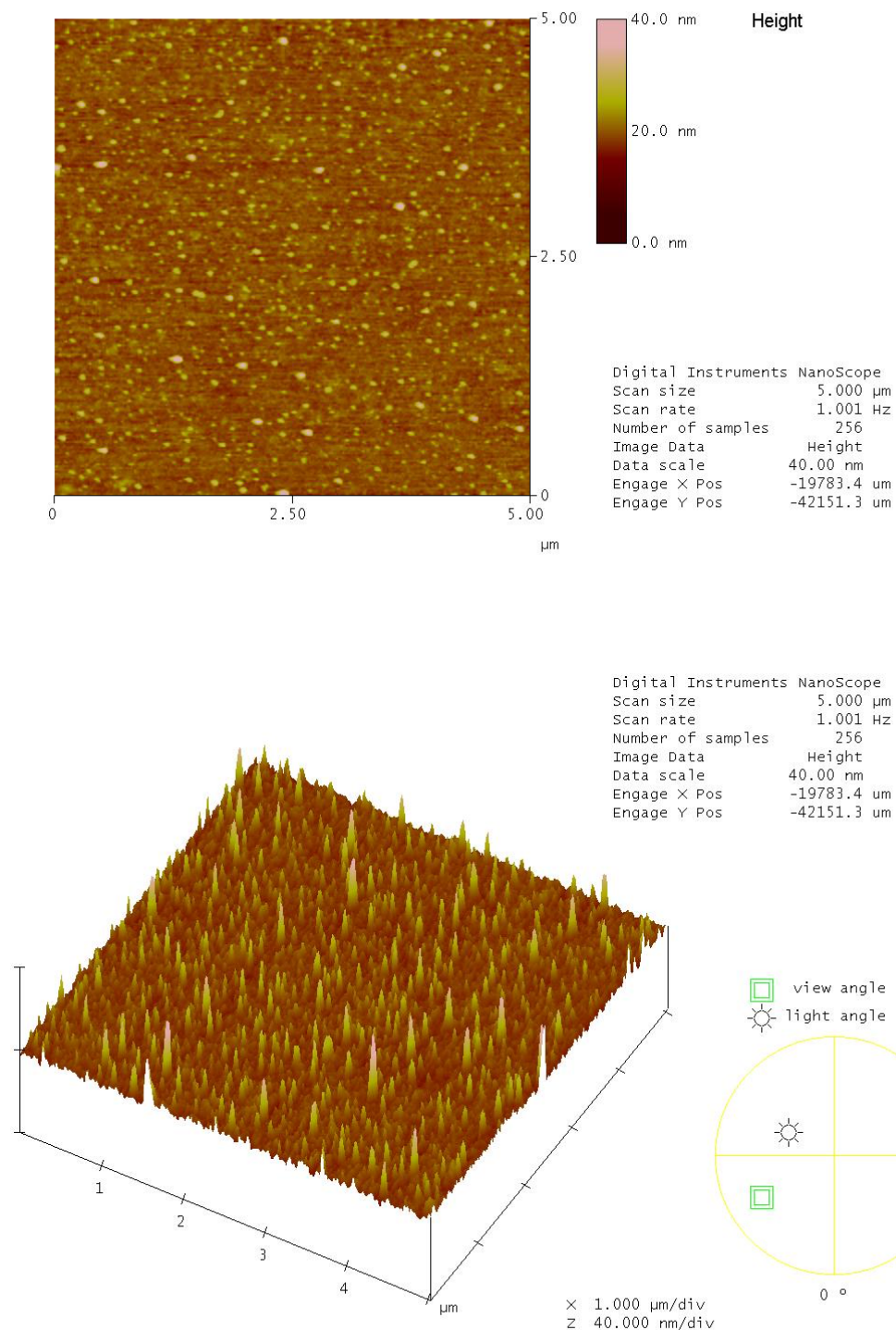


Figure S8. Additional AFM images of crown ether-coated gold surface self-assembled with randomly functional gold nanoparticles after base treatment.

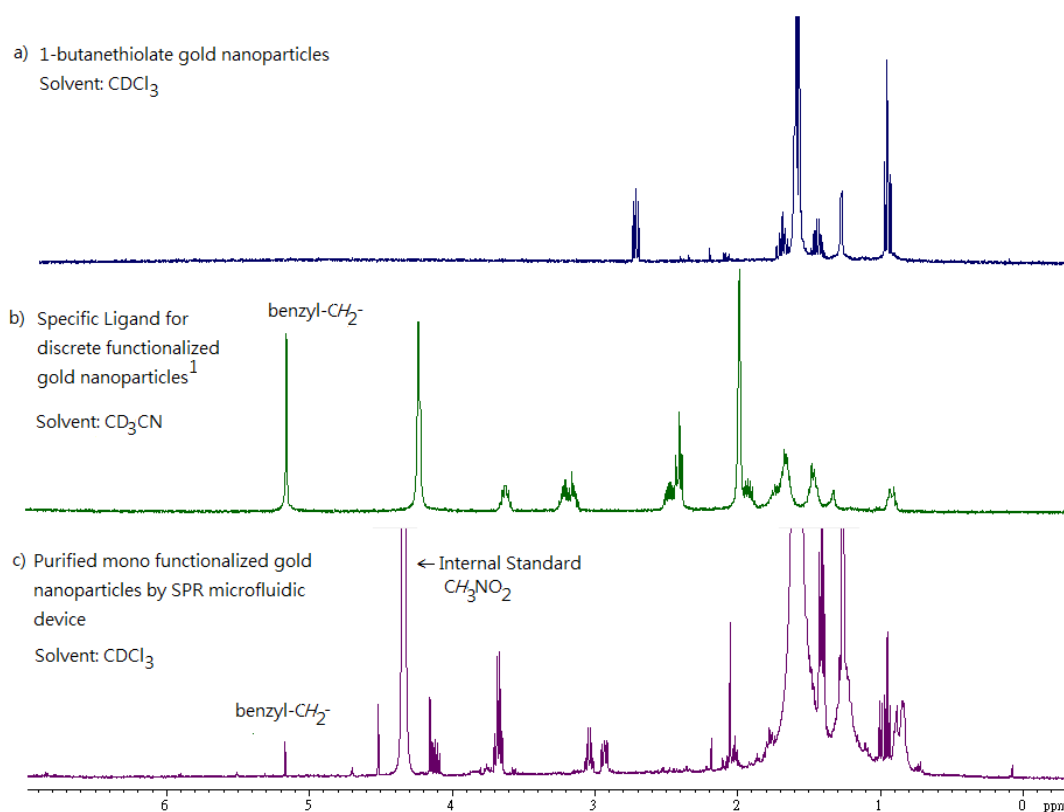


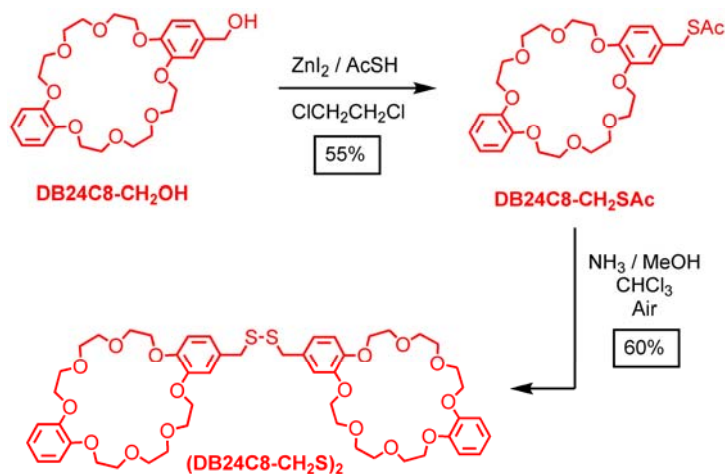
Figure S9. Stacked ¹H NMR of a) 1-butanethiolate (nonfunctional) gold nanoparticles (2 nm); b) specific ligand for discrete functionalized gold nanoparticles; and c) mono-functionalized gold nanoparticles after purification by the SPR microfluidic device. Note that the benzyl-CH₂- signal is observable in c) at δ 5.16 which is used as the reference for calculation with the internal standard of CH₃NO₂ at δ 4.33. The percentage yield was found to be 48%.^{3,4}

Chemical synthesis

General methods

25 mm × 25 mm × 1 mm N-BAF10 glass and 25 mm equilateral prism with a refractive index of 1.67003 were purchased from TEMTO Technology Co. Ltd. Polydimethylsiloxane (PDMS) was prepared by SYLGARD 184 silicone elastomer kit from Dow Corning. KDS Gemini 88 dual rate syringe pump was used. Monofunctional (secondary amine) gold nanoparticles, nonfunctional (*n*-butanethiolate) gold nanoparticles, and their crude mixtures were prepared according to the literature procedures.¹ All chemicals were purchased from Aldrich or Acros and used without further purification. Thin layer chromatography (TLC) was performed on silica gel 60 F254 (Merck). Column chromatography was performed on silica gel 60F (Merck 9385, 0.040–0.063 mm). All nuclear magnetic resonance (NMR) spectra were recorded on Bruker Avance 400 (¹H: 400 MHz; ¹³C: 101 MHz) spectrometer at 298 K and CDCl₃ was used as the solvent. The residual proton resonance signals of the non-deuterated solvents were used as reference calibration. Chemical shifts δ are reported as parts per million (ppm) for both ¹H and ¹³C NMR spectroscopies. Electrospray ionization (ESI) mass spectra were measured on a Thermo Finnigan MAT95XL mass spectrometer with CH₂Cl₂/MeOH (1:1) as the mobile phase. The reported molecular mass (*m/z*) values correspond to the most abundant monoisotopic masses. Melting points were measured on an Electrothermal 9100 digital melting point apparatus and are uncorrected.

Synthesis of New Organic Compounds



Scheme S1. Synthesis of new organic compounds **DB24C8-CH₂Sac** and **(DB24C8-CH₂S)₂**.

DB24C8-CH₂Sac. **DB24C8-CH₂OH²** (1.20 g, 2.49 mmol) was dissolved in ClCH₂CH₂Cl (10 mL) and stirred under N₂. ZnI₂ (0.91 g, 2.85 mmol) was added to the solution. Thioacetic acid (AcSH) (0.9 mL, 12.59 mmol) was added to the solution and stirred overnight at room temperature under N₂. Water was added and the product was extracted with chloroform twice. The product was then purified by flash column chromatography using hexane/ethyl acetate (1:2 v/v) gradient to 1:4 v/v as the eluent to give an off-white solid (0.73 g, 55%). Mp 68.2–69.5 °C; ¹H NMR (400 MHz, CDCl₃, δ): 2.33 (s, 3 H), 3.82–3.83 (m, 8 H), 3.88–3.92 (m, 8 H), 4.04 (s, 2 H), 4.10–4.15 (m, 8 H), 6.75–6.81 (m, 3 H), 6.85–6.90 (m, 4 H); ¹³C NMR (101 MHz, CDCl₃, δ): 30.5, 33.4, 69.5, 69.6, 70.0, 70.0, 71.4, 113.9, 114.0, 114.1, 114.5, 121.5, 121.7, 130.7, 148.2, 149.0, 149.0; HRMS(ESI, *m/z*): [*M* + Na]⁺ calcd for C₂₇H₃₆O₉SNa, 559.1972; found, 559.1980 (100%).

(DB24C8-CH₂S)₂. Minimum amount of chloroform was added to dissolve **DB24C8-CH₂Sac** (0.10 g, 0.19 mmol) with stirring. Ammonia in methanol (2 M, 15 mL, 901 mmol) was then added to the solution. After three days reaction in air, water was added and the product was extracted with chloroform twice. The excess of solvent of the organic layer was evaporated in *vacuo* to give an off-white solid (0.11 g, 60%). Mp 109.3–109.7 °C; ¹H NMR (400 MHz, CDCl₃, δ): 3.54 (s, 4 H), 3.79–3.80 (m, 16 H), 3.88–3.89 (m, 16 H), 4.09–4.12 (m, 16 H), 6.73–6.78 (m, 6 H), 6.83–6.88 (m, 8 H); ¹³C NMR (101 MHz, CDCl₃, δ): 43.1, 69.3, 69.4, 69.8, 69.8, 71.2, 113.6, 114.0, 114.9, 130.3, 148.3, 148.7, 148.8; HRMS(ESI, *m/z*): [*M* + Na]⁺ calcd for C₅₀H₆₆O₁₆S₂Na, 1009.3684; found, 1009.3671 (100%).

References:

1. Chak, C.-P.; Xuan, S.; Mendes, P. M.; Yu, J. C.; Cheng, C. H. K.; Leung, K. C.-F. *ACS Nano* **2009**, *3*, 2129–2138.
2. Leung, K. C.-F.; Mendes, P. M.; Magonov, S. N.; Northrop, B. H.; Kim, S.; Patel, K.; Flood, A. H.; Tseng, H.-R.; Stoddart, J. F. *J. Am. Chem. Soc.* **2006**, *128*, 10707–10715.
3. Hostetler M. J.; Wingate J. E.; Zhong C. J.; Harris J. E.; Vachet R. W.; Clark M. R.; Londono J.D.; Green S. J.; Stokes J. J.; Wignall G. D.; Glish G. L.; Porter M. D.; Evans N. D.; Murray R. W. *Langmuir* **1998**, *14*, 17–30.
4. Shaffer A. W.; Worden J. G.; Huo Q. *Langmuir* **2004**, *20*, 8343–8351.

^{13}C NMR spectrum of **DB24C8-CH₂Sac**.

